Collaborators:
Lisa Gächter
Chuyao Tong
Rebekka Garreis
Max Ruckriegel
Christoph Adam
Lara Ostertag
Jonas Gerber
Annika Kurzmann
Marius Eich
Klaus Ensslin
hBN supply:
Kenji Watanabe
Takashi Taniguchi
Theory:
Angelika Knothe
Vladimir Fal'ko

Graphene-based nanostructures

Part I: Gate-defined devices in bilayer graphene

Thomas Ihn

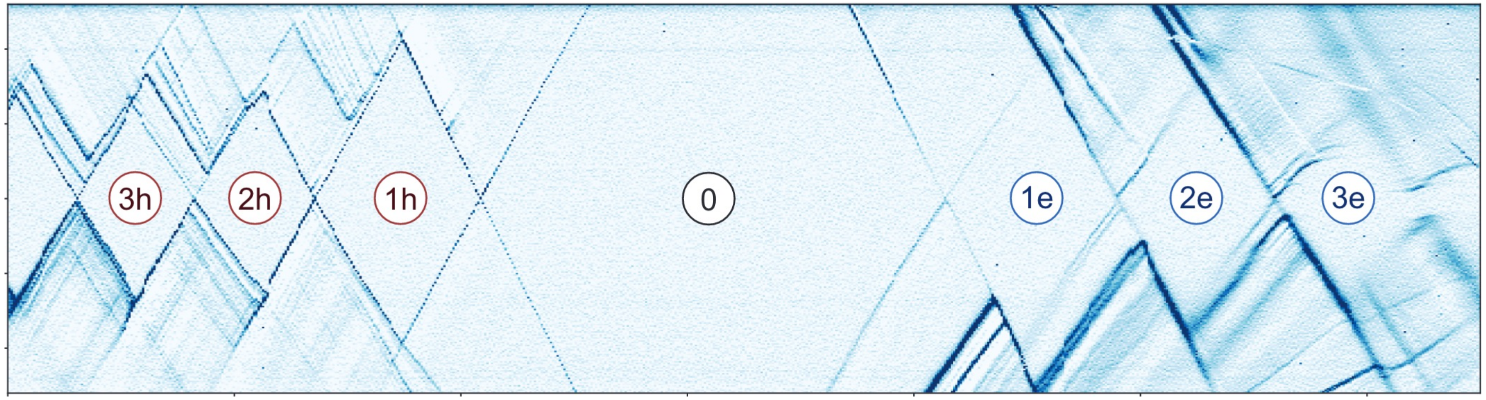

QSIT Quantum Science and Technology
National Centre of Competence in Research

ETH Eidgenössische Technische Hochschule Zürich

Outline

- Fabrication
- Gate-defined quantum point contacts
- Gate-defined single quantum dots
- Quantum dots with charge sensors
- Double quantum dots: spin- and valley-blockade
- Double quantum dot with charge sensor

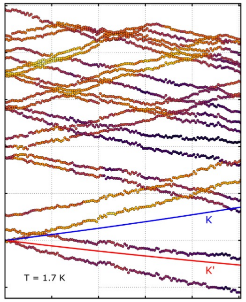

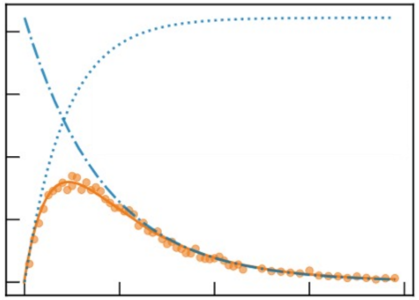

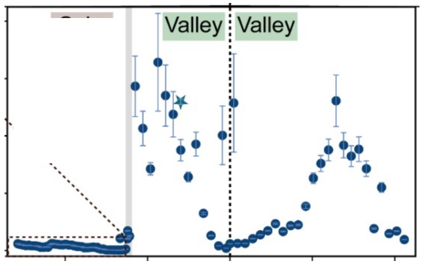

Mechanical exfoliation

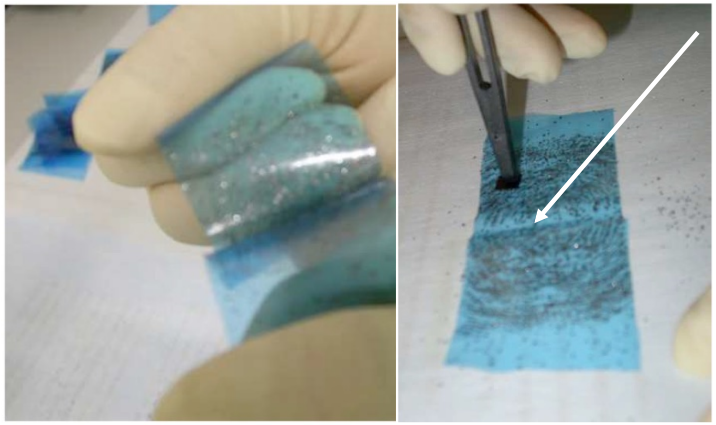

K.S. Novoselov, A.K. Geim *et al.*
Science **306**, 666 (2004)

Optical microscope

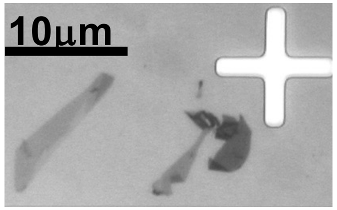

Raman spectroscopy

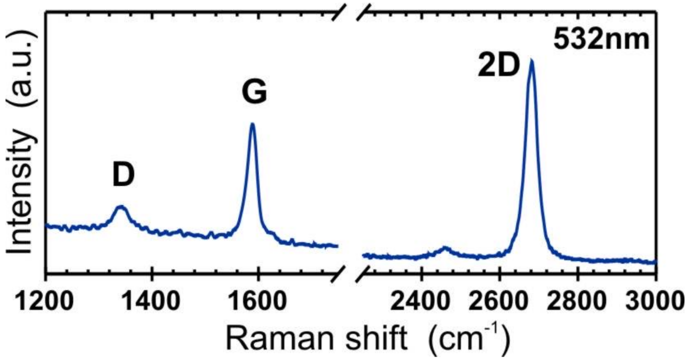

Graphene:
one to three atomic layers thick
almost no volume, only surface
made with a "dirty" method

Graphite:
usually more than 10 layers

hBN:
usually 20–30 nm thick

Flake hunting

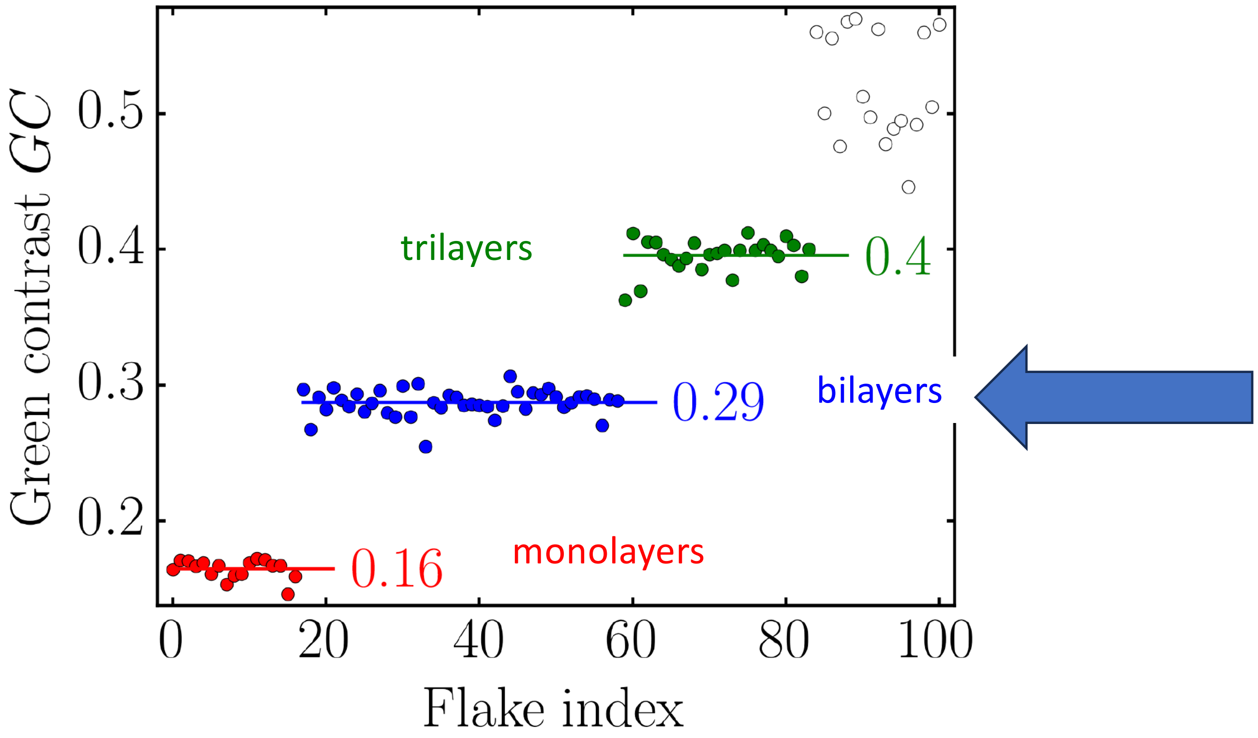

M. Eich
PhD Thesis,
ETH Zurich (2018)

Si wafers with
90 nm SiO_2

See also:
Ying Ying Wang *et al*, Nanotechnology **23**, 495713 (2012)

Dry transfer technique

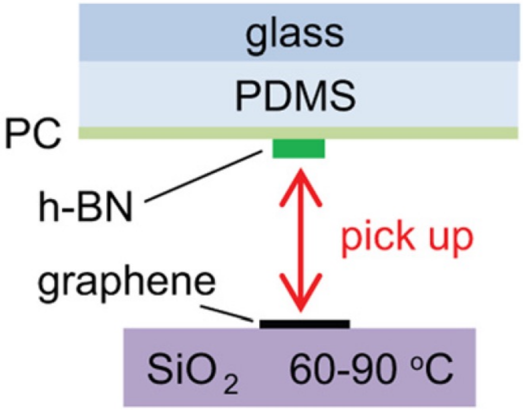

P.J. Zomer *et al*, Appl. Phys. Lett. **105**, 013101 (2014)

PC: Polycarbonate
PDMS: Polydimethylsiloxane

Pick-up performed in glove box with Ar atmosphere
using a micromanipulator

Annealing in Ar/H_2 atmosphere at 350°C

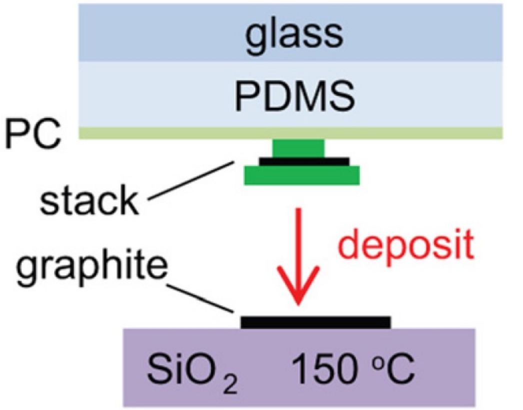

Stacking layers

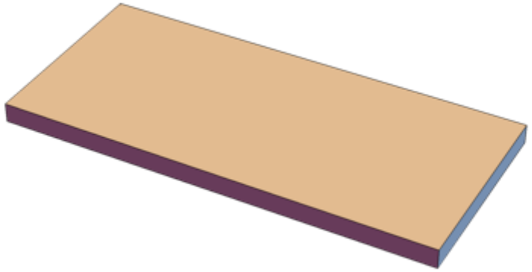

1. Si/SiO$_2$ substrate
(2004, Geim, Novoselov)

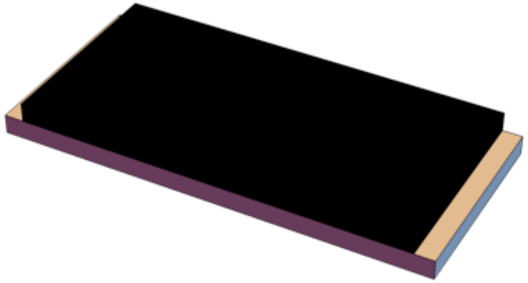

2. Graphite back gate
(2013, Hunt)

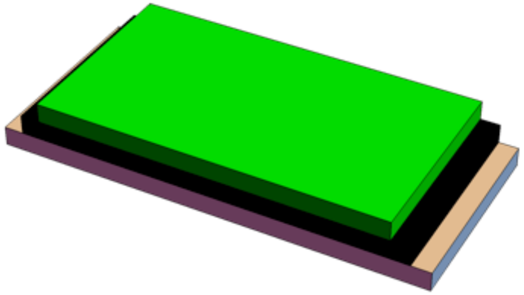

3. hBN insulator
(2010, Dean)

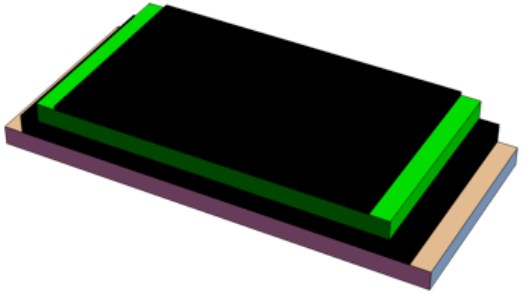

4. Bilayer graphene
(2004, Geim, Novoselov)

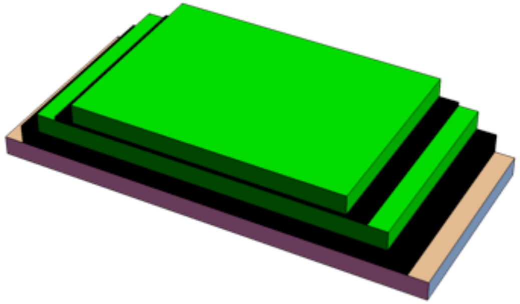

5. hBN insulator
(2013, Wang)

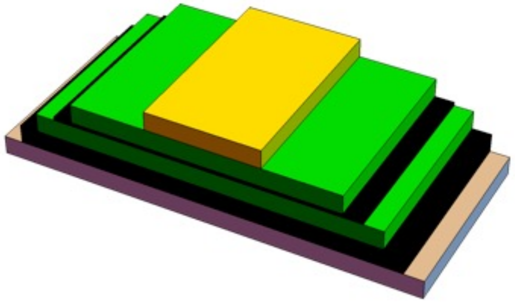

6. Au top gate

Edge contacting

L. Wang *et al*, Science **342**, 614 (2013)

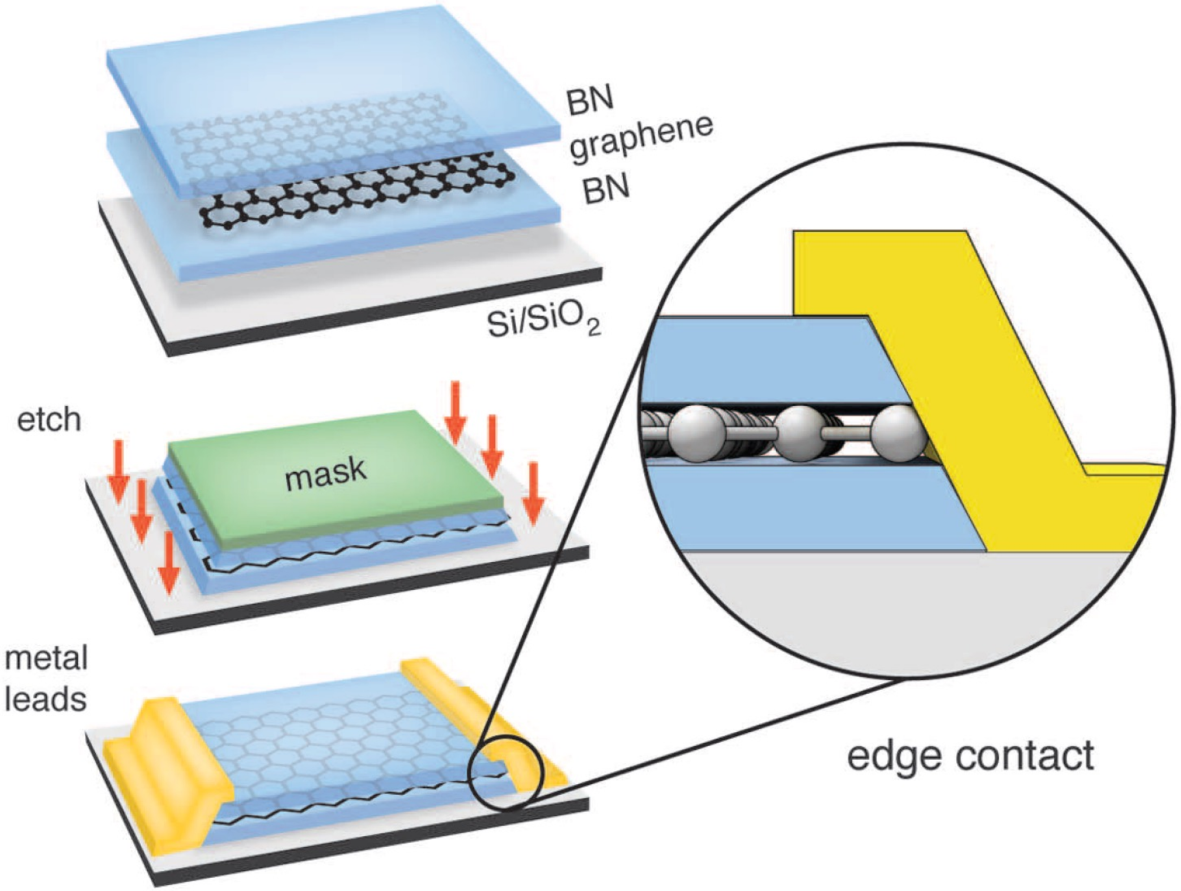

Breaking inversion symmetry: gate-induced band gap

Tight binding model:

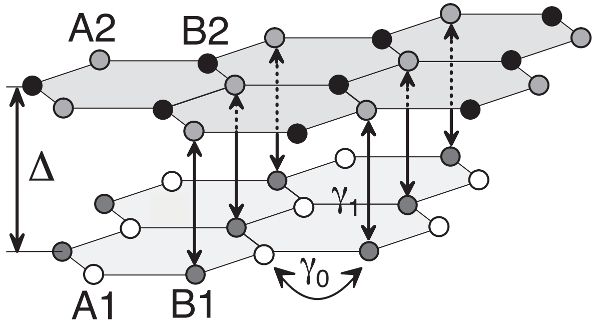

McCann, Koshino,
Rep. Prog. Phys. **76**, 056503 (2013)

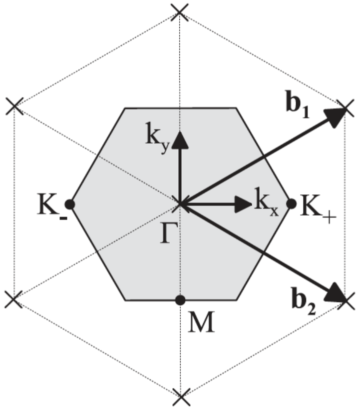

Conduction band

Valence band

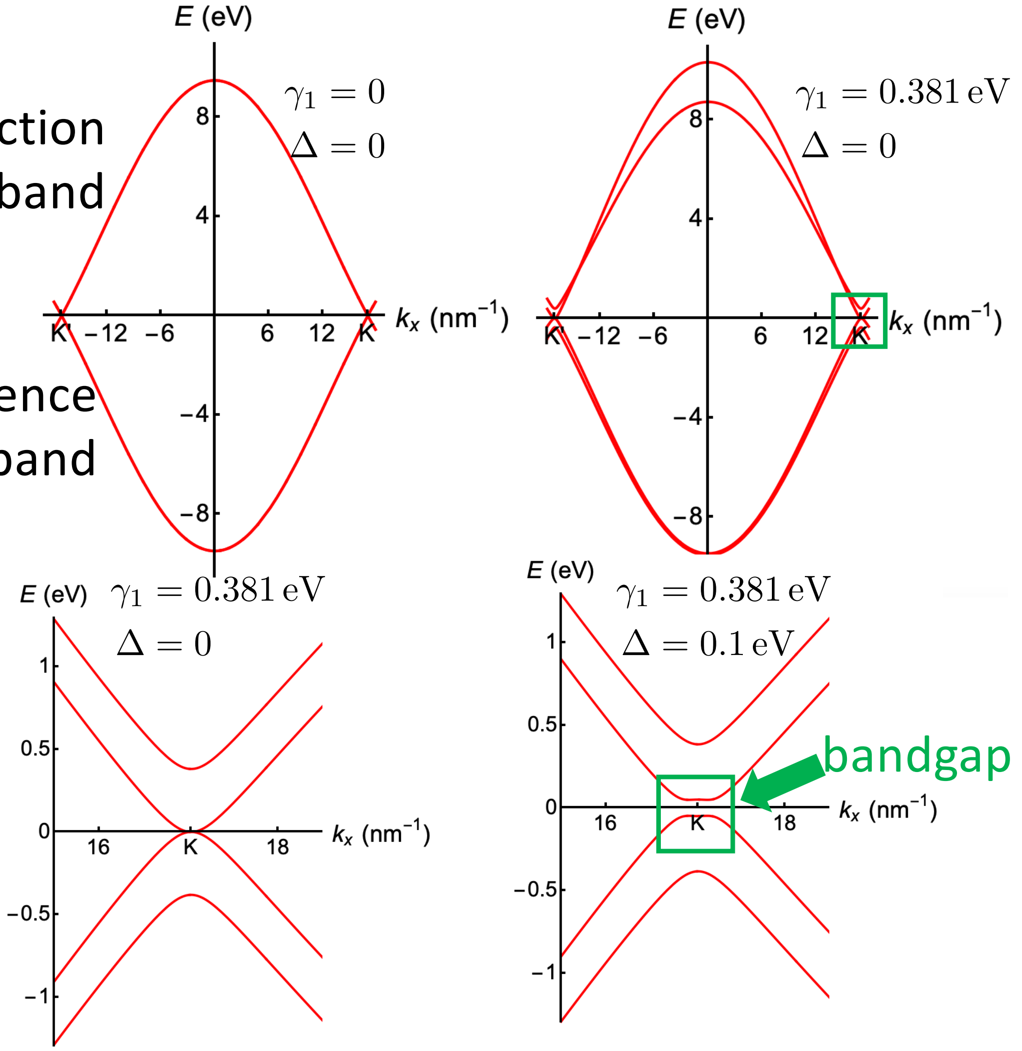

bandgap

Experimental evidence for the band gap

Oostinga *et al*,
Nature Materials **7**, 151 (2008).

Bilayer graphene resistance

T = 1.7 K

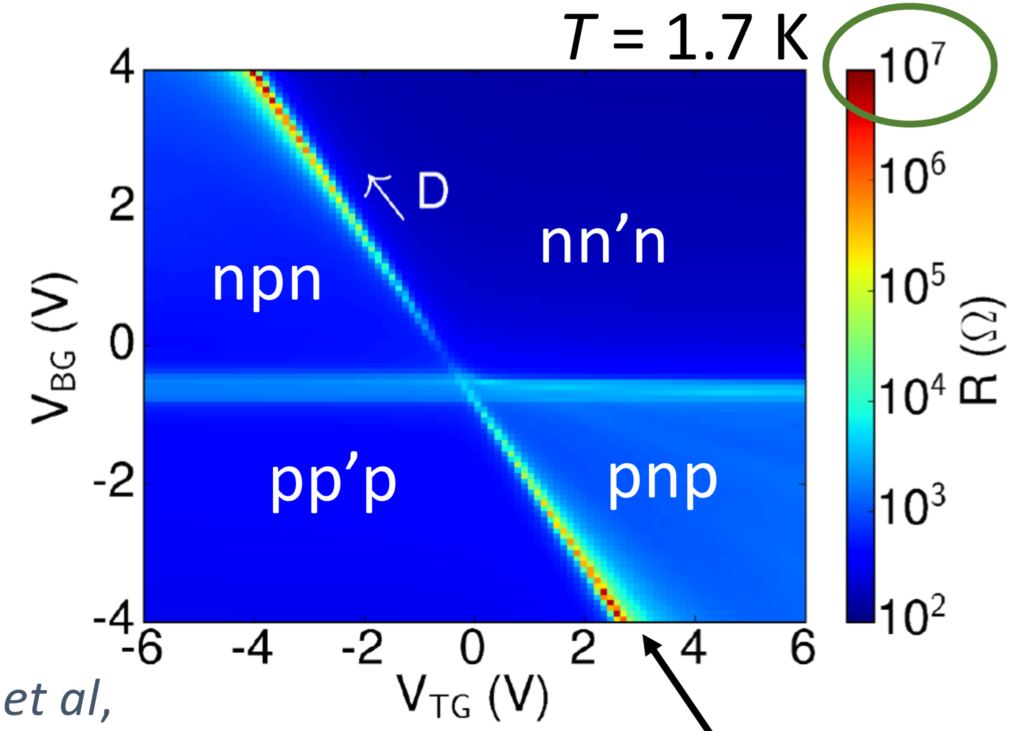

Overweg *et al*,
Nano Lett **18**, 553 (2018).

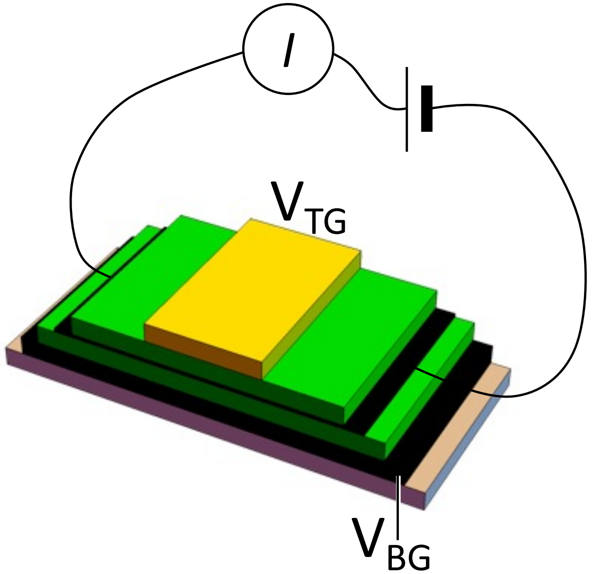

Below top gate: E_F in the gap

Conducting channel using split gate

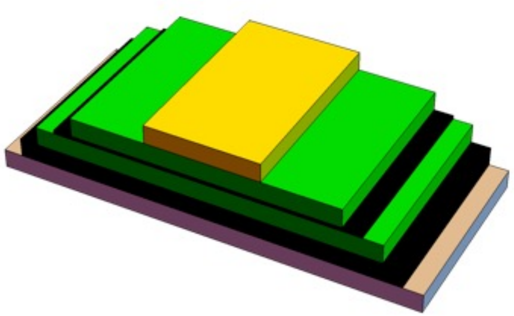

Homogeneous gate

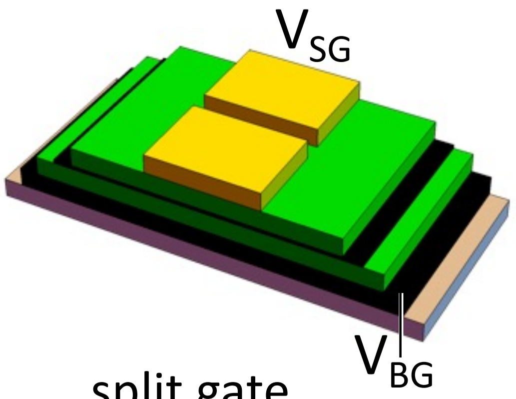

split gate

Sample resistance

T = 1.7 K

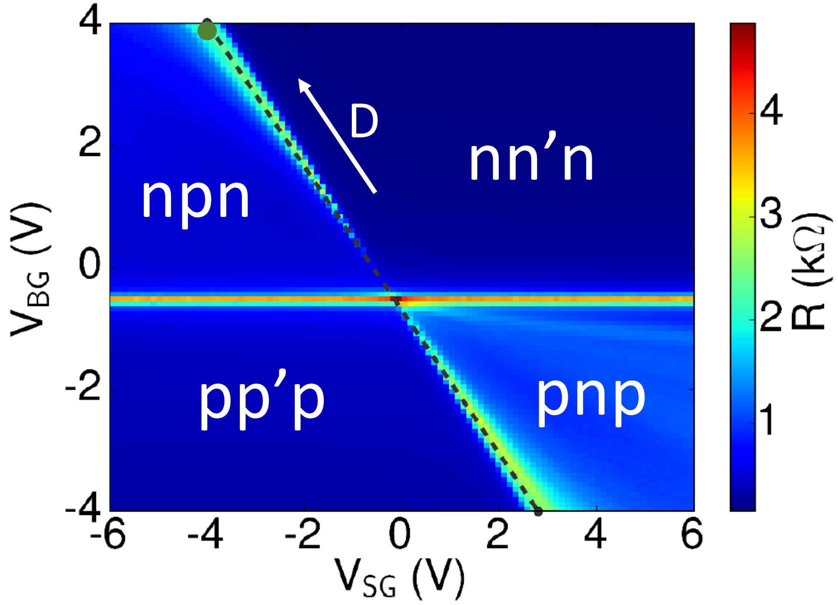

H. Overweg *et al*, Nano Letters **18**, 553 (2018).

Local density control in the channel

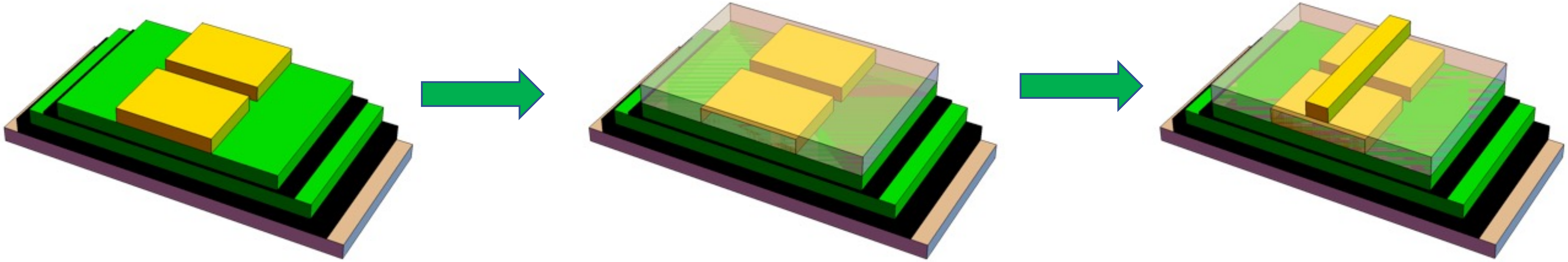

Split gate

AlOx insulator (ALD)

Finger gate (Au)

H. Overweg *et al*, Nano Letters **18**, 553 (2018).

Quantized conductance

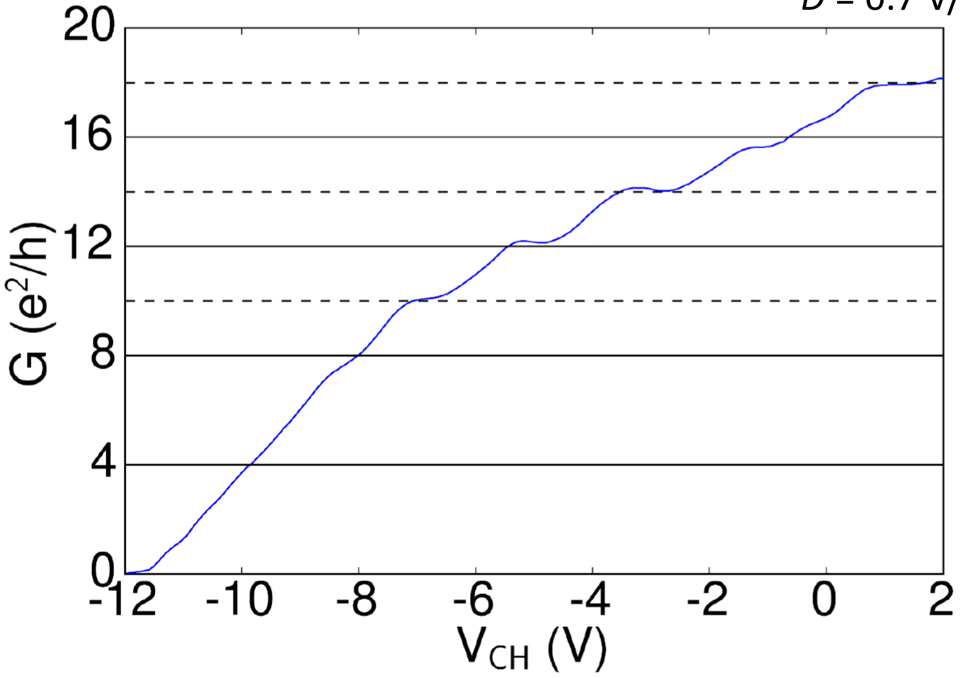

T = 1.7 K
D = 0.7 V/nm

series resistance
of 200 Ω subtracted

H. Overweg *et al*, Nano Lett. **18**, 553 (2018)

Depletion of the channel

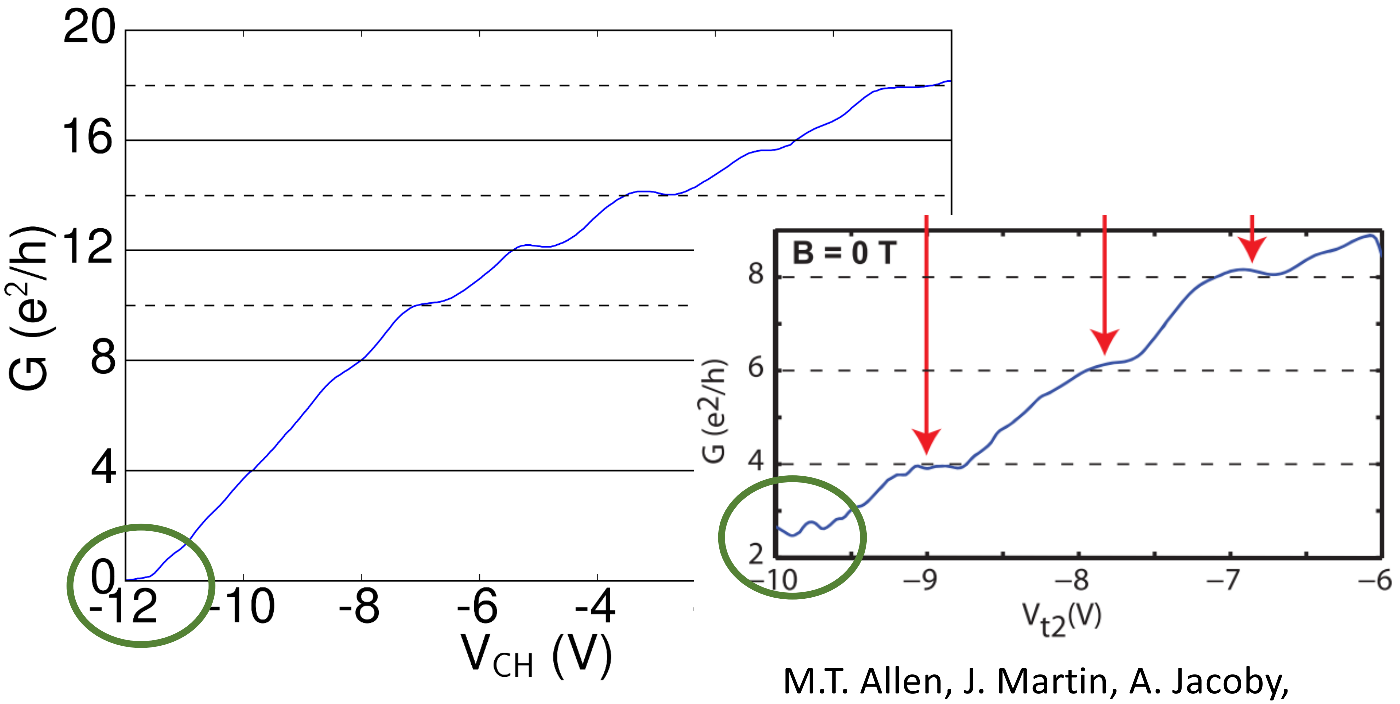

Pinch-off resistance: 10 MΩ

M.T. Allen, J. Martin, A. Jacoby,
Nature Comm. **3**, 934 (2012)

Magnetic depopulation of subbands

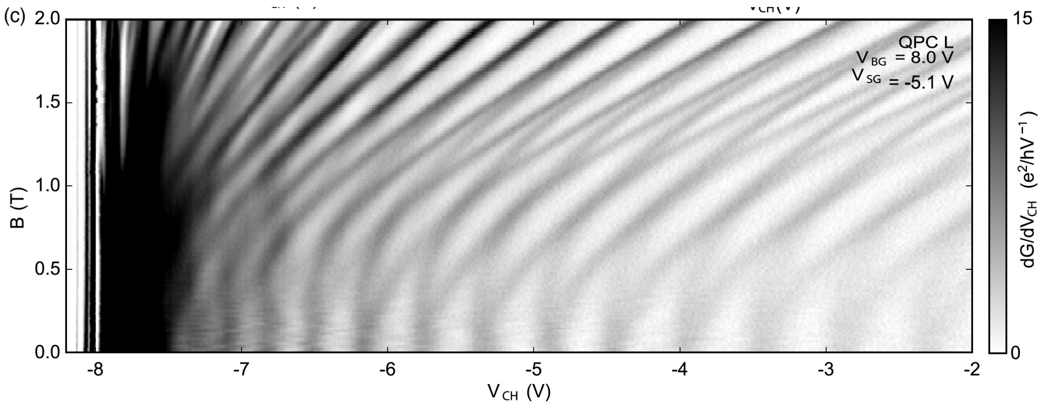

Experiment:
measured differential conductance

H. Overweg *et al.*, Phys. Rev. Lett. **121**, 257702 (2018)

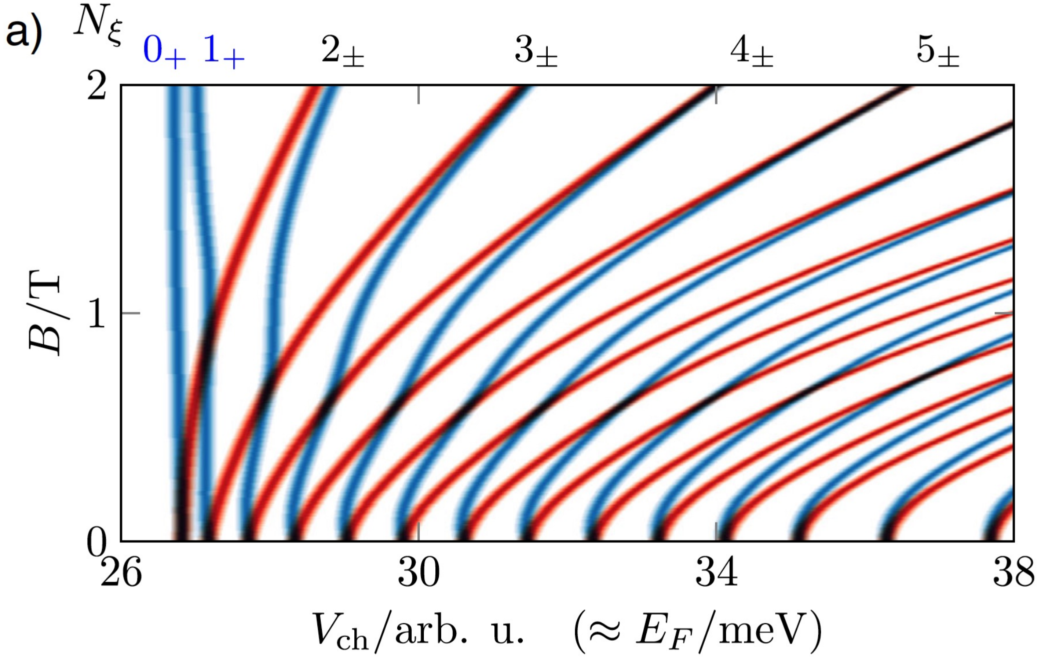

Theory:
calculated differential conductance

K states
K’ states

Topology in bilayer graphene

Berry curvature near the K-point

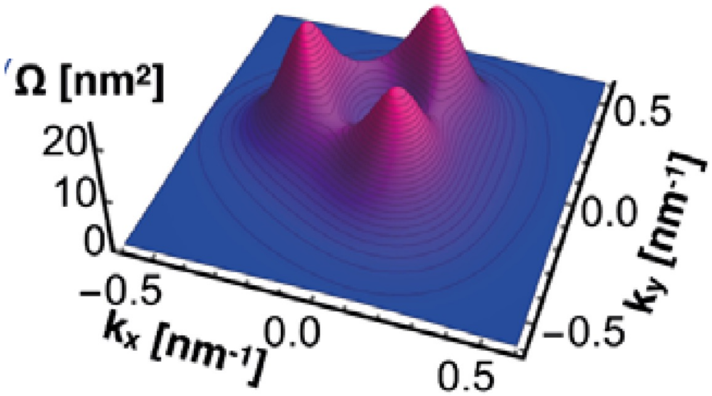

Three-fold symmetry due to trigonal warping (γ_3 parameter in tight-binding model)

H. Overweg *et al.*, Phys. Rev. Lett. **121**, 257702 (2018)

Leads to magnetic moment of wave packets

Opposite sign for K and K’ → Valley splitting at low *B*

Why graphene quantum dots?

Common qubit materials:

GaAs
Si
Ge

Common problems:

Hyperfine interaction
Spin-orbit interaction
Charge noise
Material inhomogeneities
Strain

What graphene has to offer

Naturally 2D
High abundance
Sustainable
99% Nuclear Spin Free
Very small spin-orbit interaction
hBN as extremely good insulator
Gate-tunable band gap (BLG)
Berry-curvature effects
Gate-defined quantum dots
Spin qubits
Valley qubits

Gate-defined quantum dots in bilayer graphene

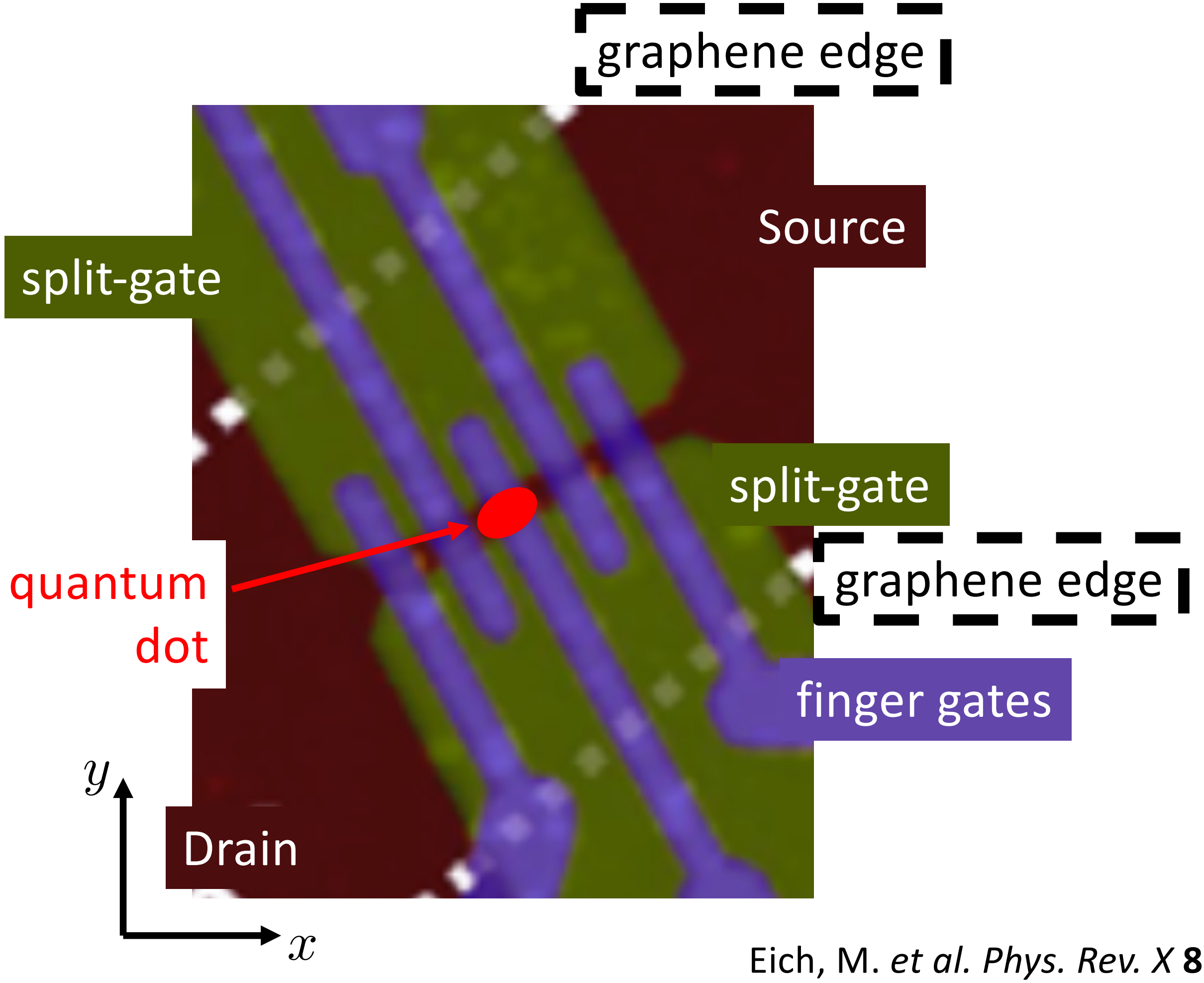

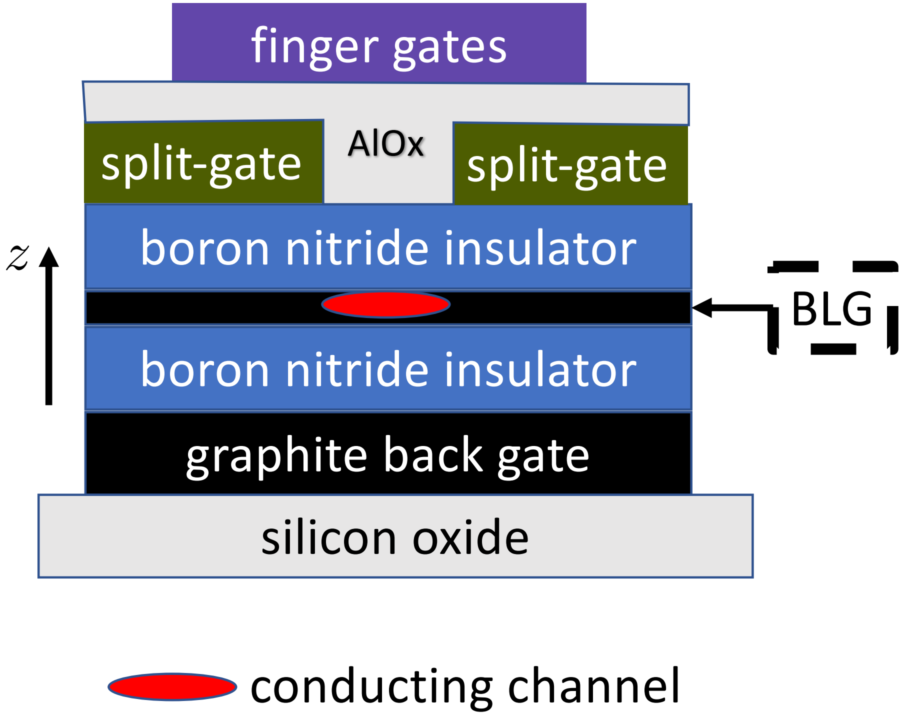

Eich, M. *et al. Phys. Rev. X* **8**, 031023 (2018).

Eich, M. *et al. Phys. Rev. X* **8**, 031023 (2018).

Valley and spin states

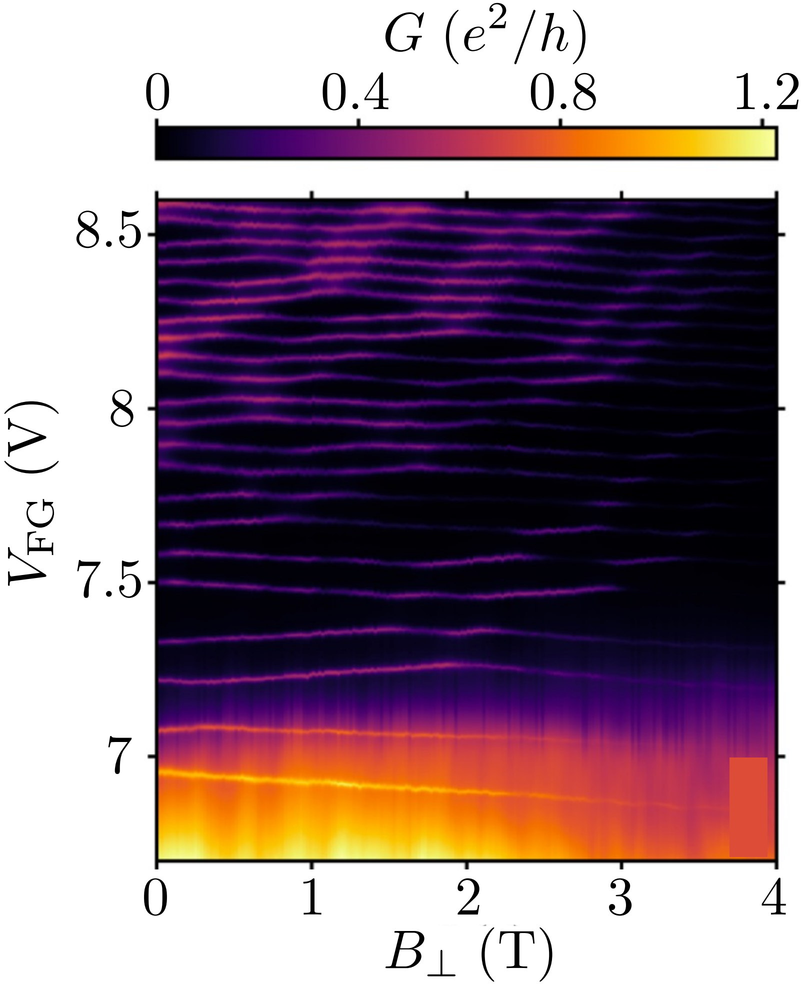

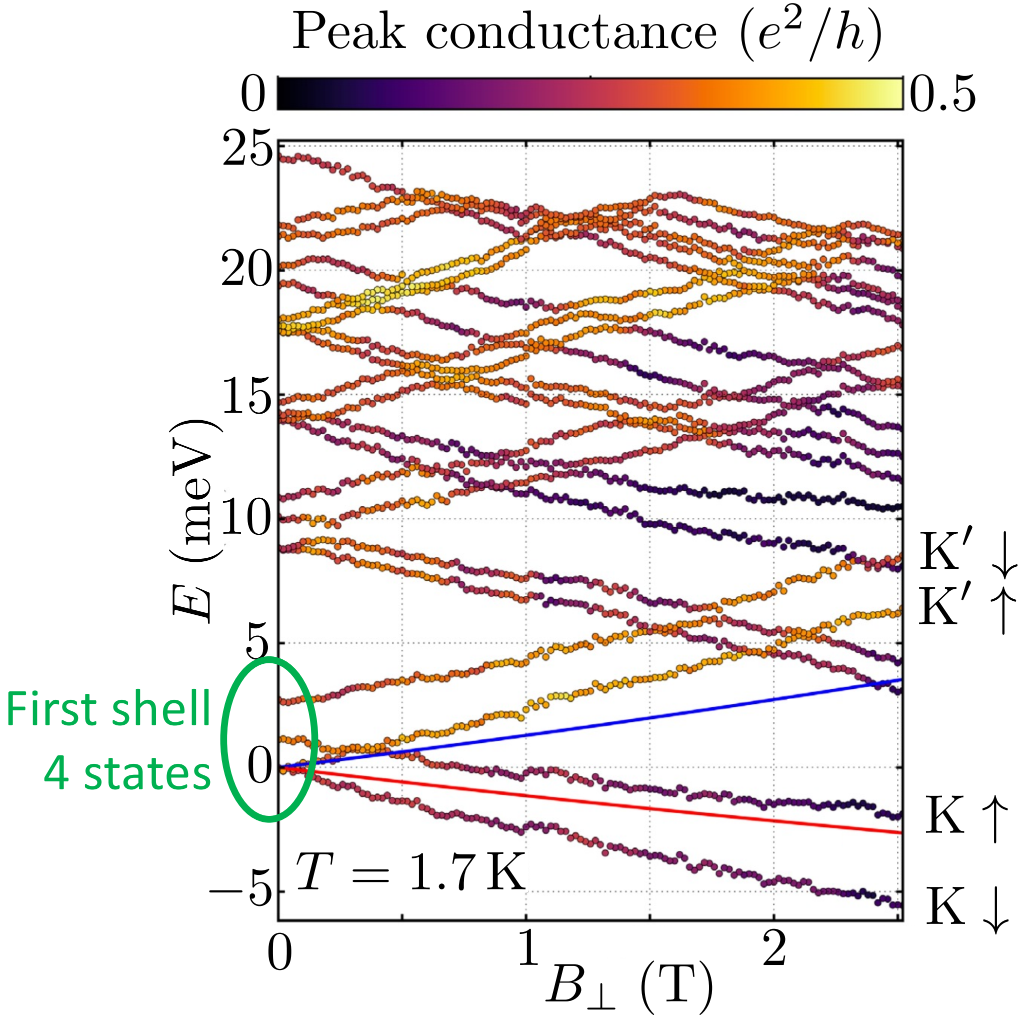

Tunable valley splitting: effect of Berry curvature

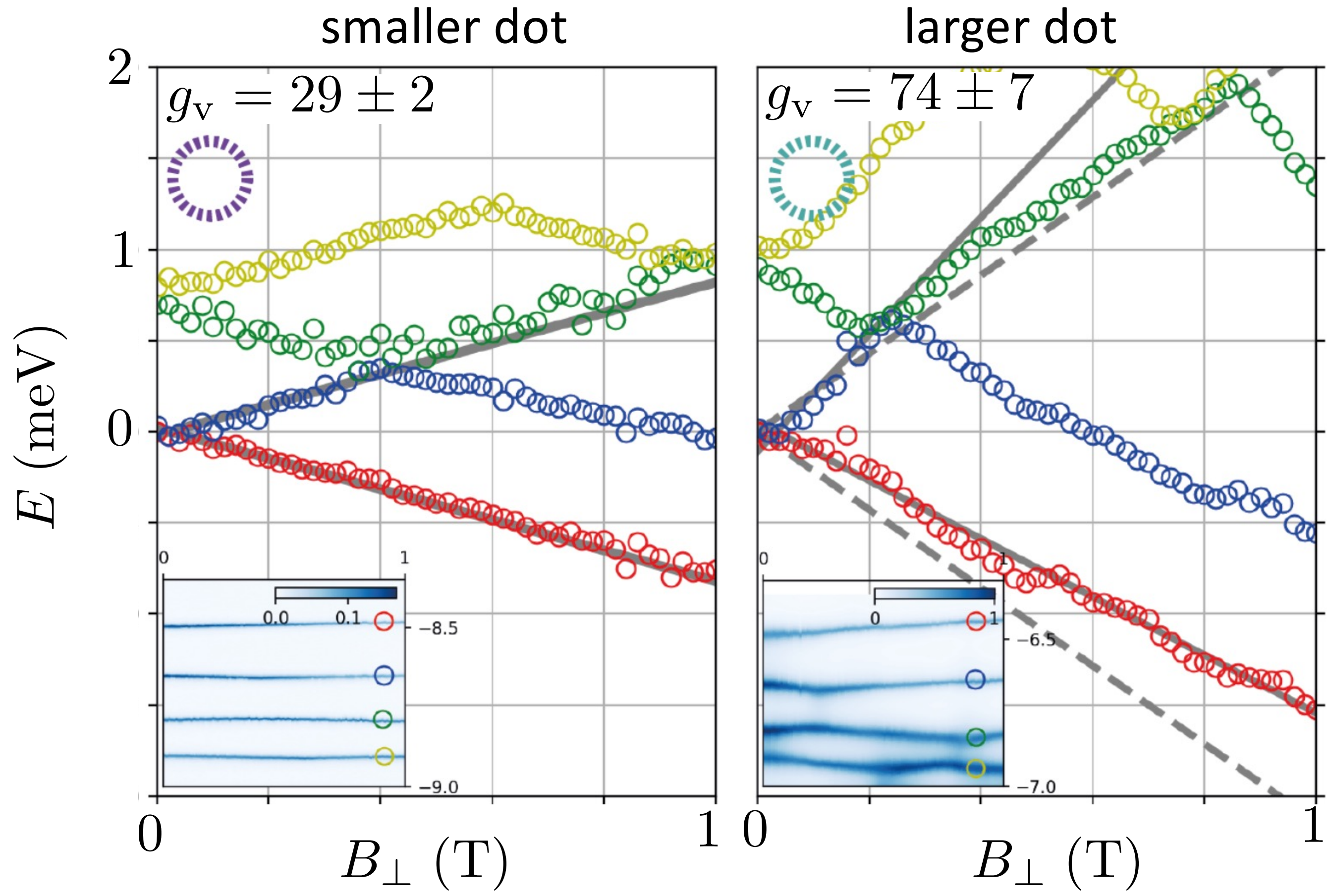

$$\boxed{\Delta E_v = g_v \mu_B B_\perp}$$

Magnetization

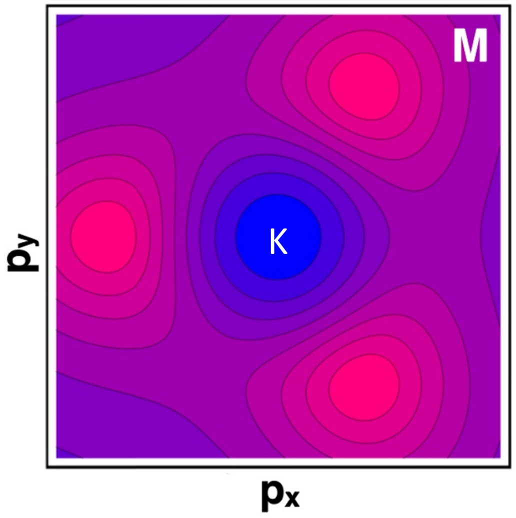

Tong, C. *et al*,
Nano Lett. **21**, 1068–1073 (2021).

Quantum dot with integrated charge sensor

Single quantum dot
with charge sensor

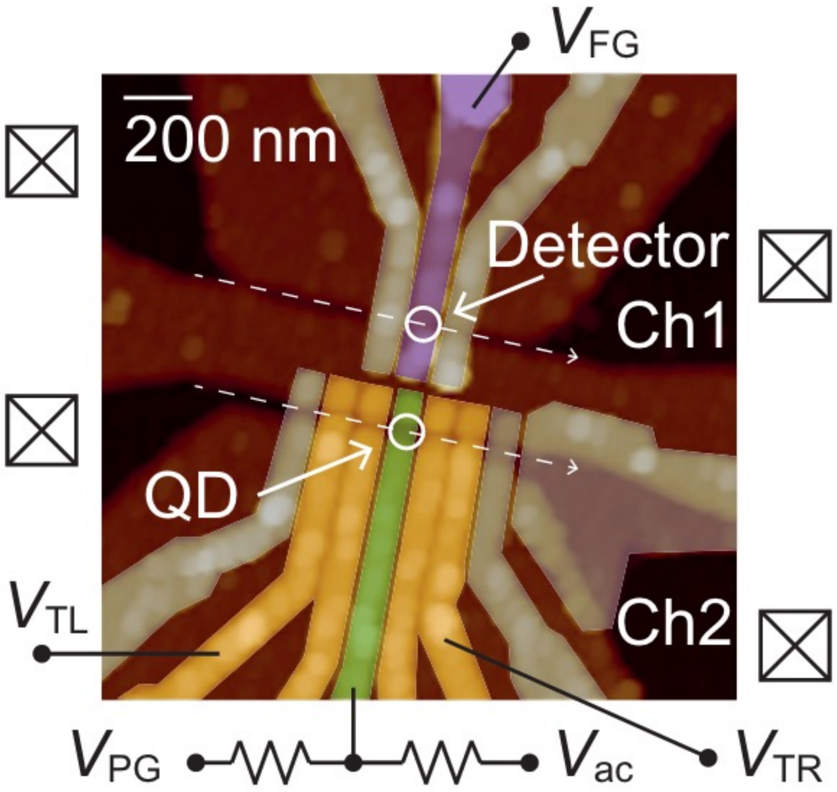

Gächter, L. M. and Garreis R. *et al,*
PRX Quantum **3**, 020343 (2022).

Spin-orbit coupling

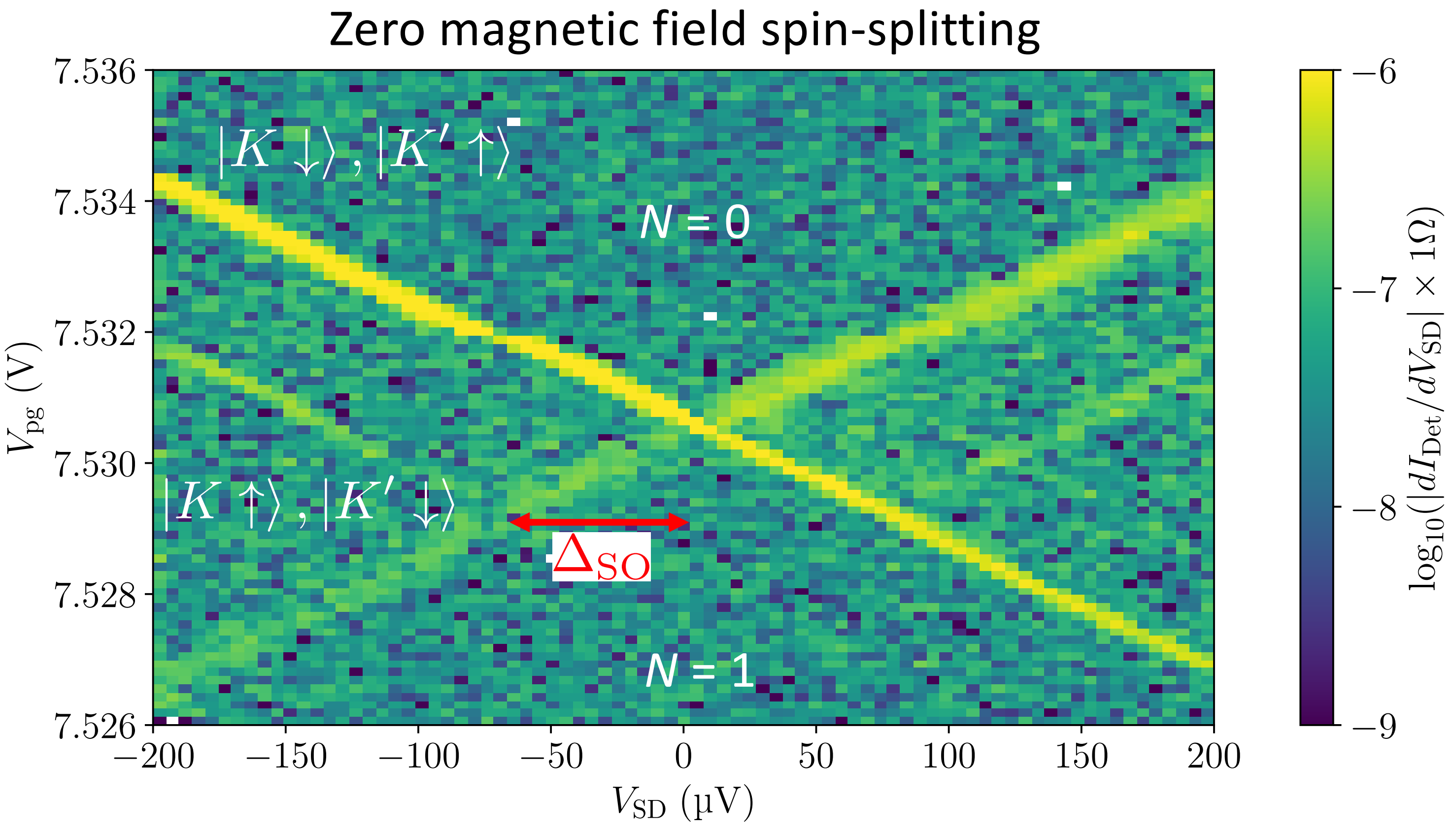

Kane, C. L. & Mele,
Phys. Rev. Lett. **95**, (2005).

$$\boxed{\Delta_{\mathrm{SO}} = (73 \pm 5)\,\mu\mathrm{eV}}$$

Data: Christoph Adam
(unpublished)

see also:
Kurzmann, A. *et al*,
Nat Commun **12**, 6004 (2021).

One-hole energy spectrum (perp. field)

Data: Christoph Adam
(unpublished)

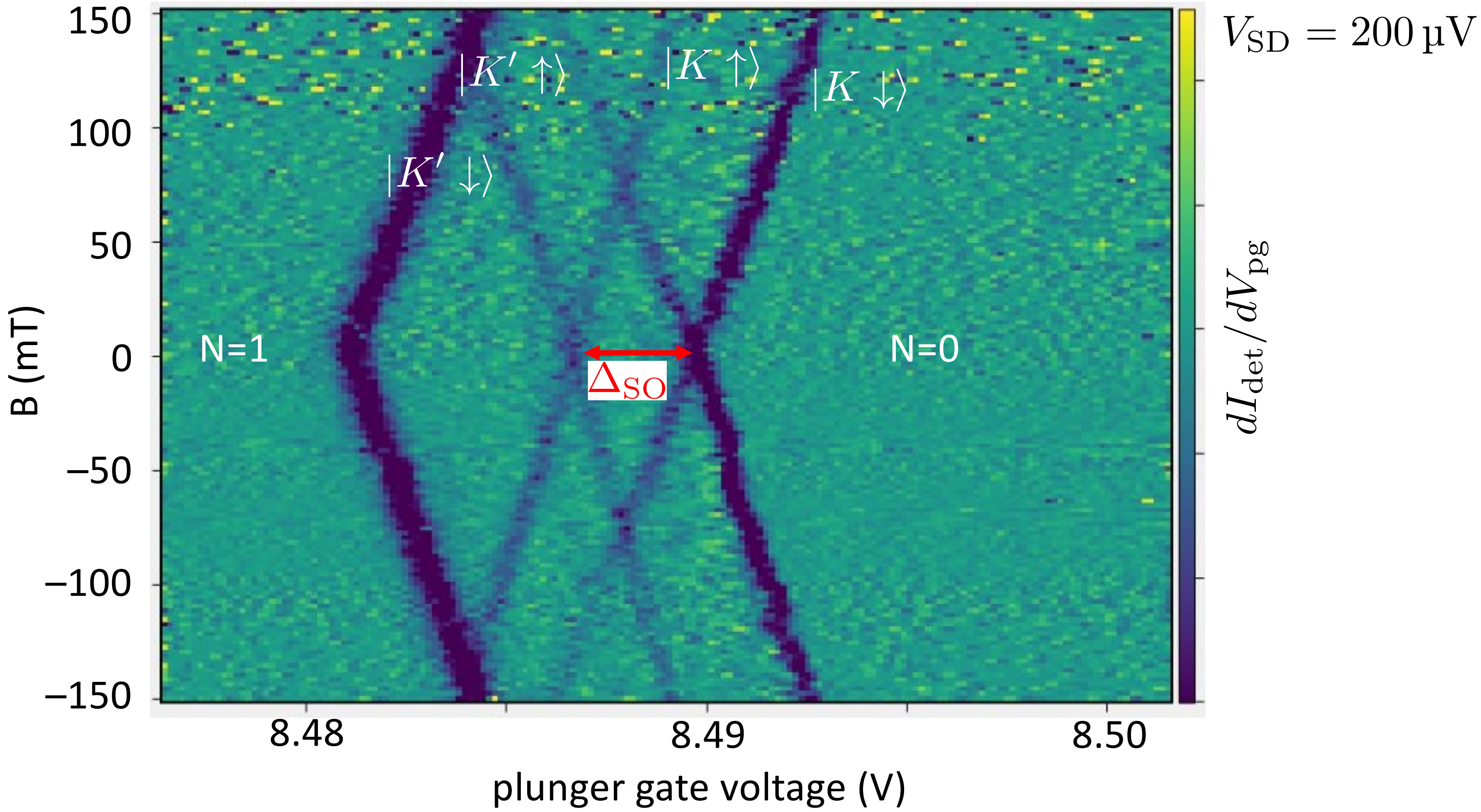

One-hole energy spectrum

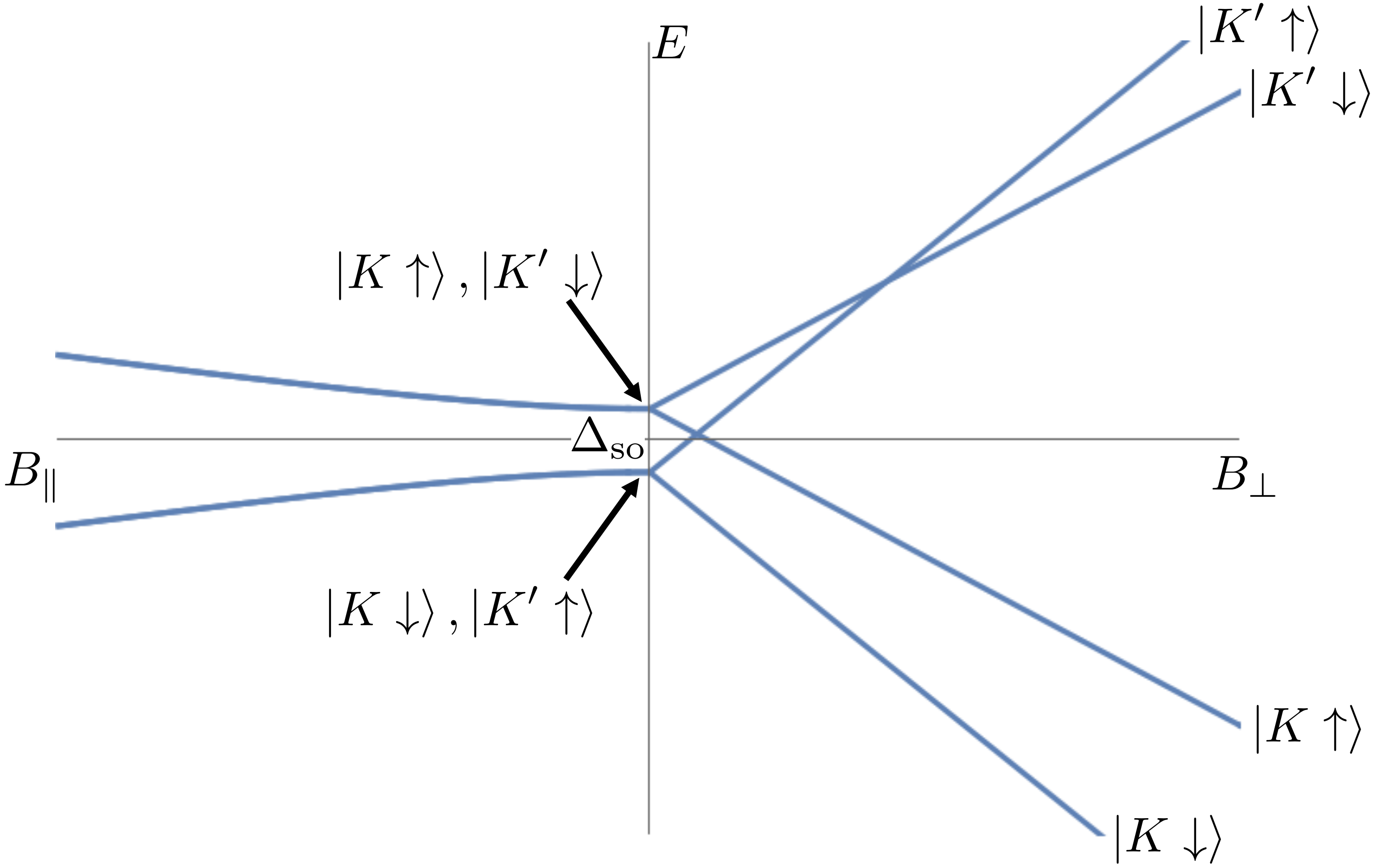

Spin-relaxation measurement:
Elzerman read-out

Technique:
Elzerman, J. M. *et al,*
Nature **430**, 431–435 (2004).

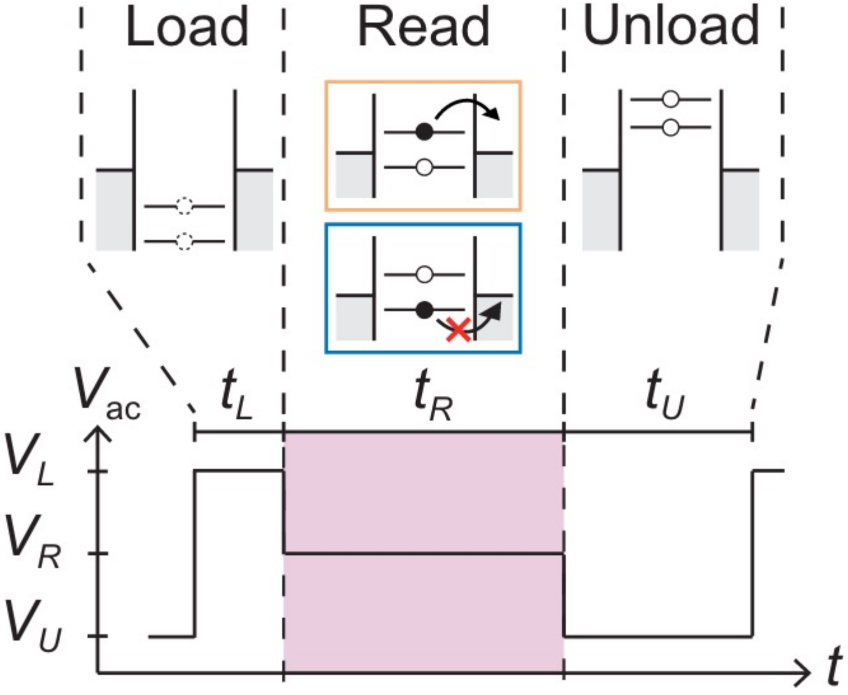

Gächter, L. M. and Garreis R. *et al,*
PRX Quantum **3**, 020343 (2022).

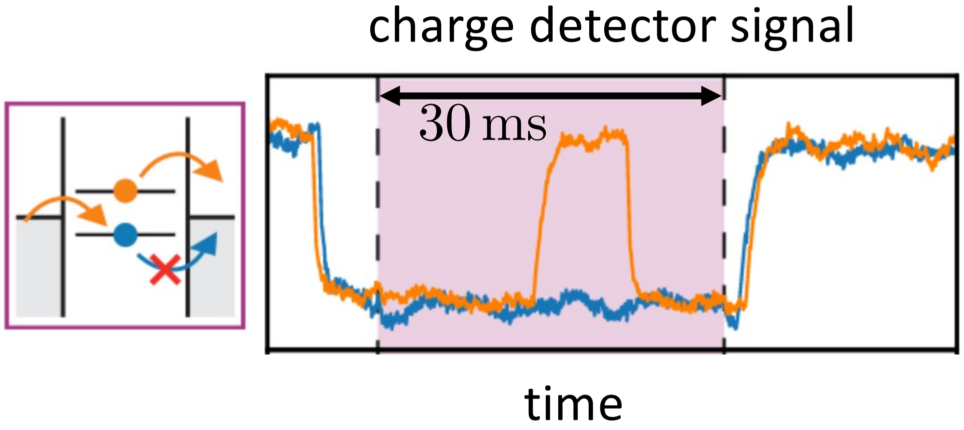

Spin-relaxation times

Gächter, L. M. and Garreis R. *et al,*
PRX Quantum **3**, 020343 (2022).

Histogram of detector voltage
during read phase

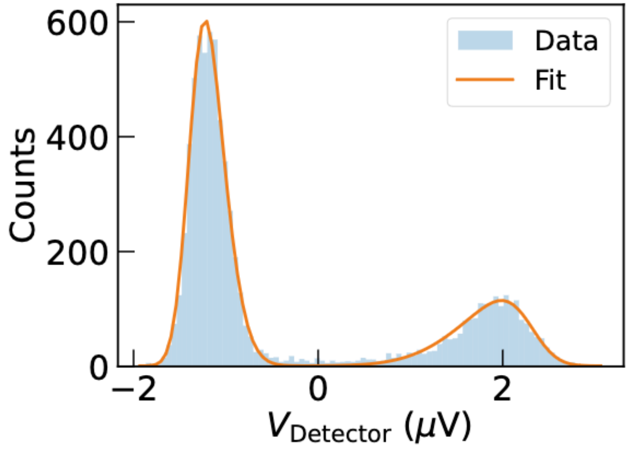

Number of detected blips
as a function of load time

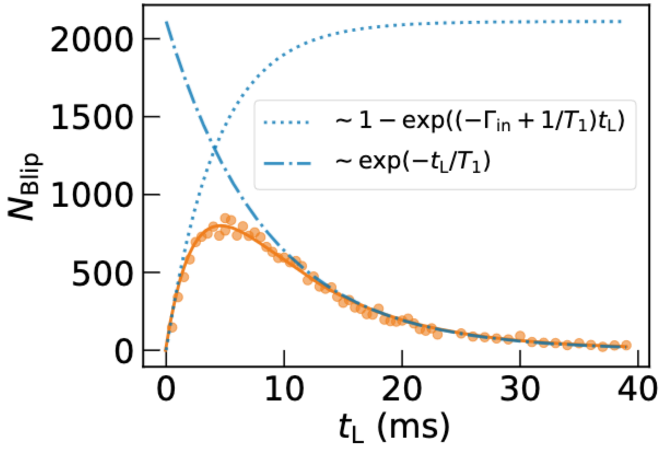

Spin decay rates
for different magnetic fields

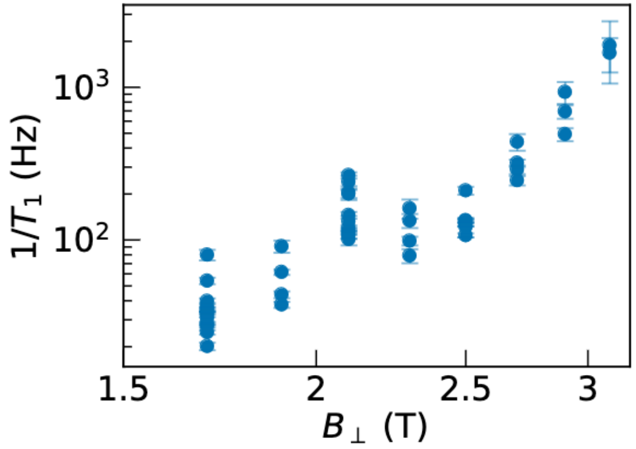

Electrical read-out fidelity: >99%

Largest spin relaxation time: $T_1 = 50\,\mathrm{ms}$ at $B = 1.7\,\mathrm{T}$

Two-hole ground and excited states

Kurzmann, A. *et al*,
Phys. Rev. Lett. **123**, 026803 (2019).

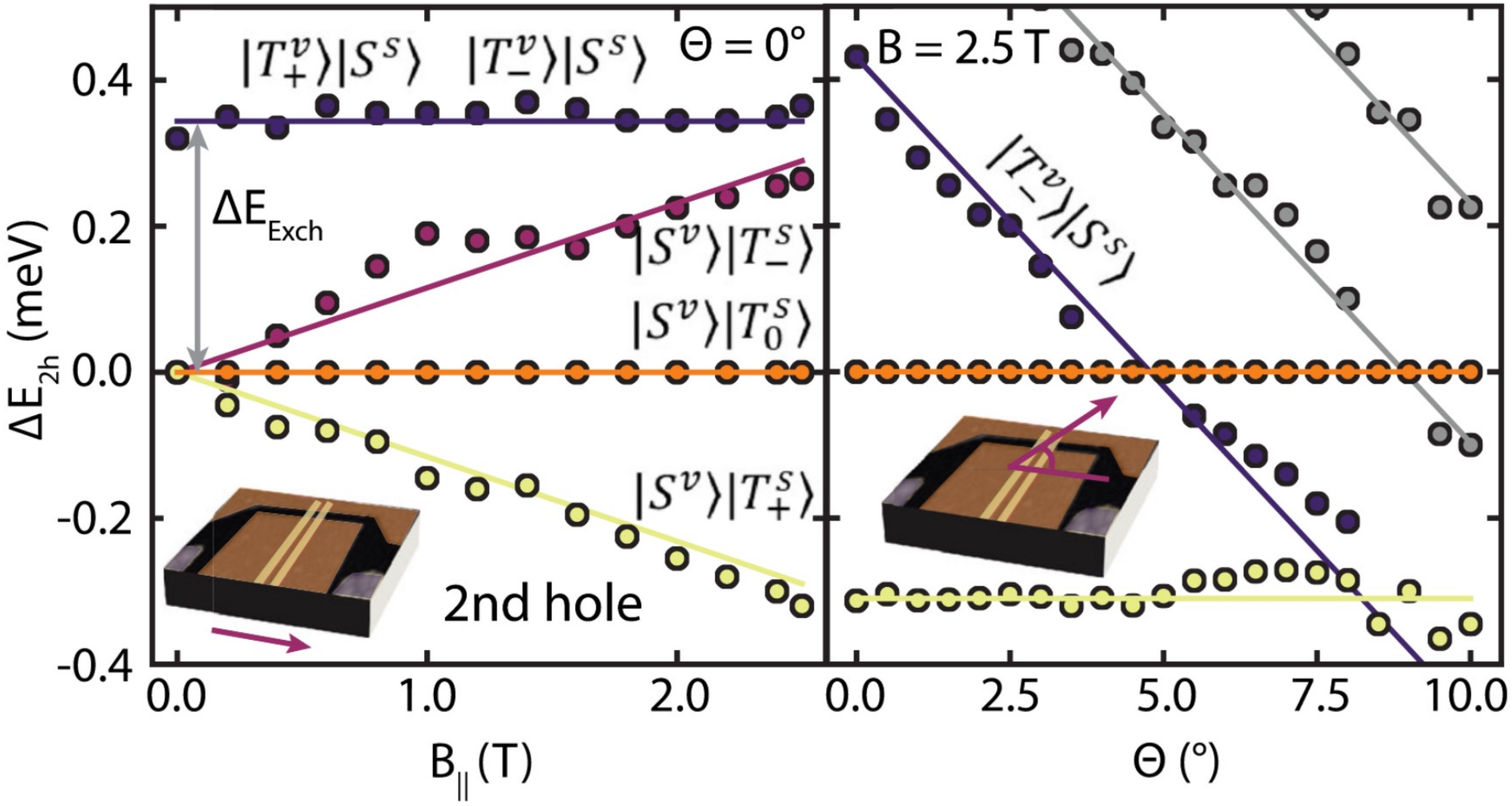

Two-hole ground state:
Spin triplet!

Triplet–Singlet splitting

$$\boxed{\Delta E_{\mathrm{exch}} = 350\,\mathrm{\mu eV}}$$

at $B = 0$

Single-dot two-hole energy spectrum

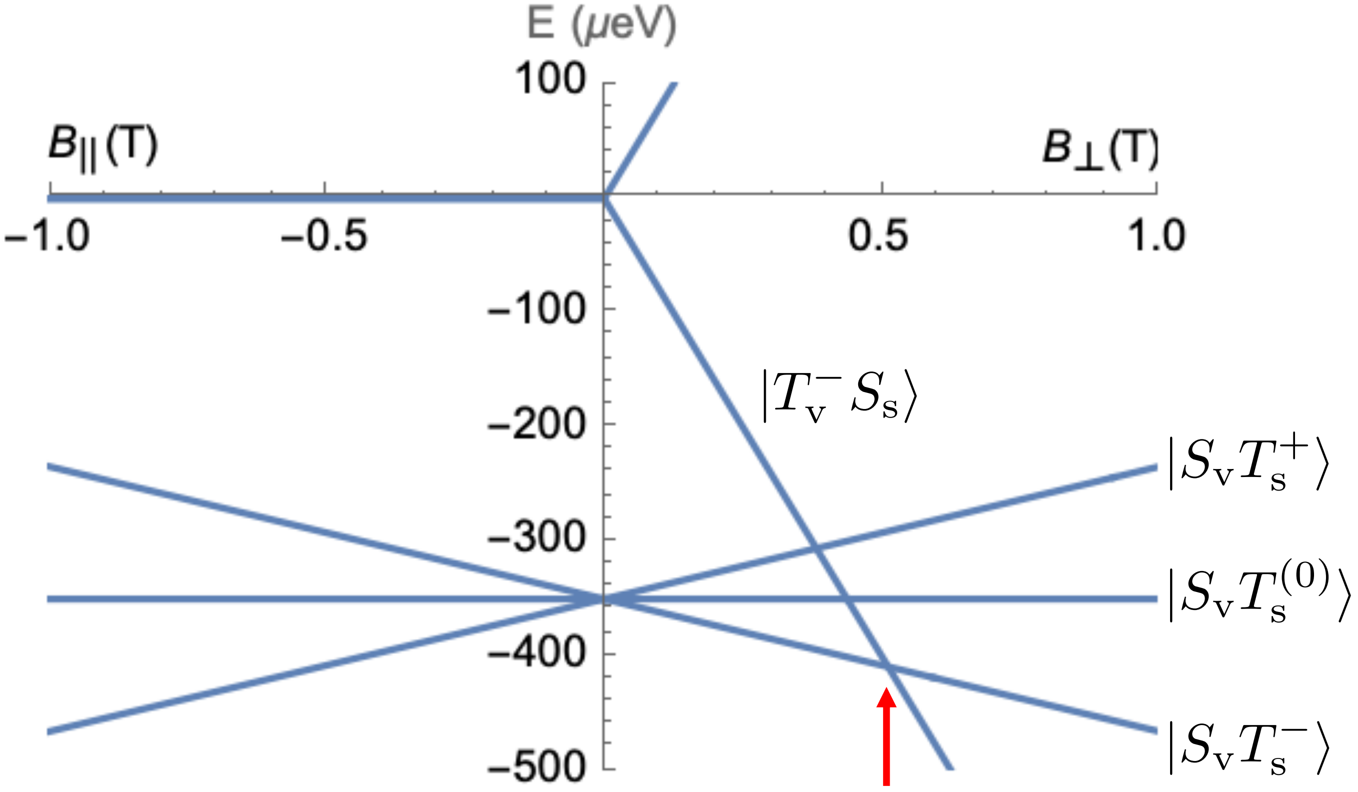

Triplet-Singlet
Transition

Pauli valley blockade at B = 0 T

V_{SD} = -1 mV
no blockade

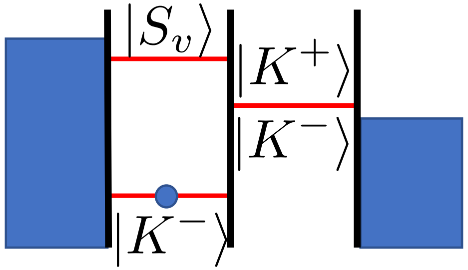

V_{SD} = +1 mV
valley
singlet-triplet
blockade

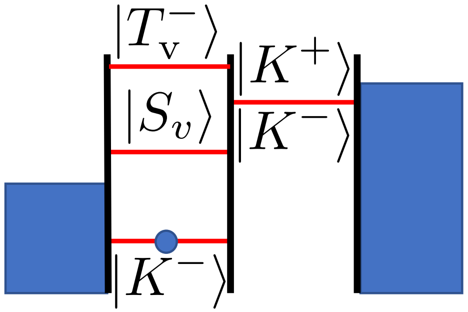

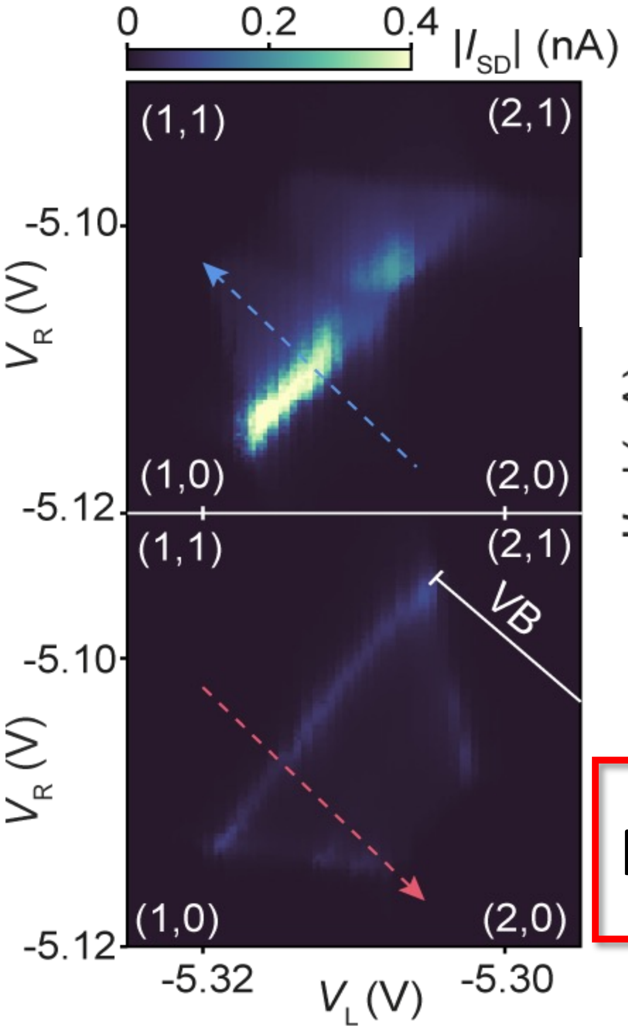

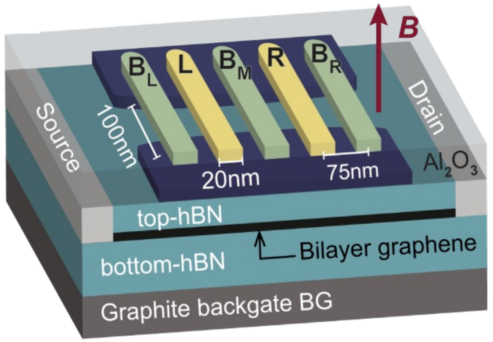

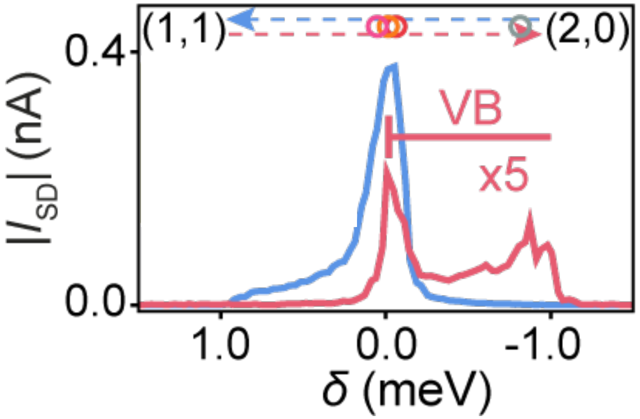

Pauli valley-blockade

Tong, C. *et al, Phys. Rev. Lett.* **128**, 067702 (2022).

Pauli spin blockade at B = 800 mT

V_{SD} = -1 mV

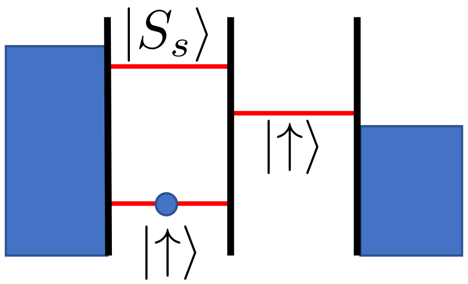

V_{SD} = +1 mV
spin
singlet-triplet
blockade

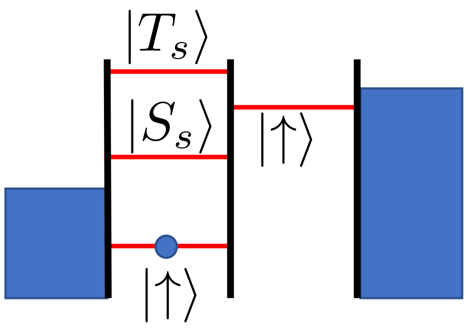

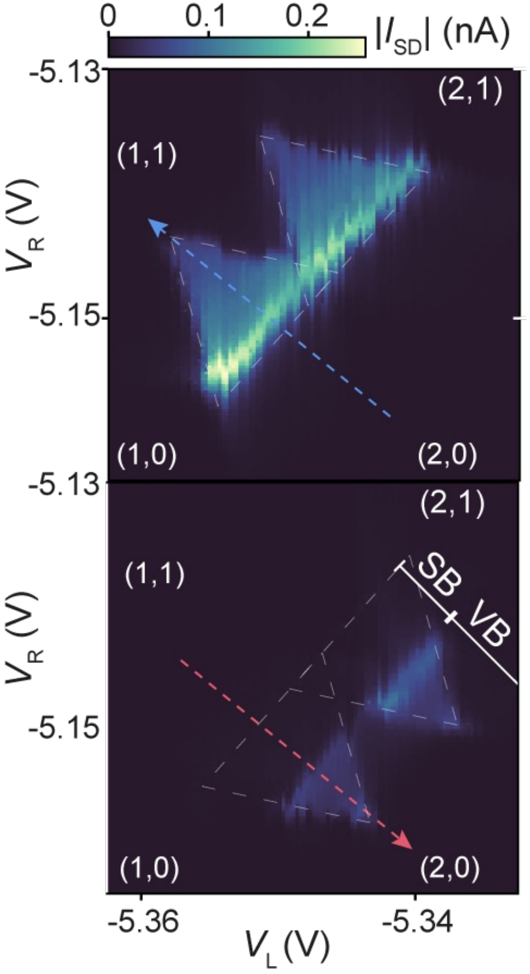

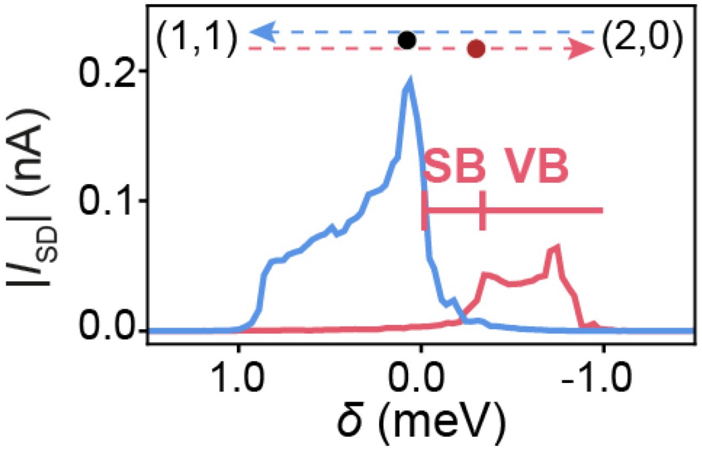

Pauli spin-blockade

Tong, C. *et al, Phys. Rev. Lett.* **128**, 067702 (2022).

Double quantum dot with charge sensor

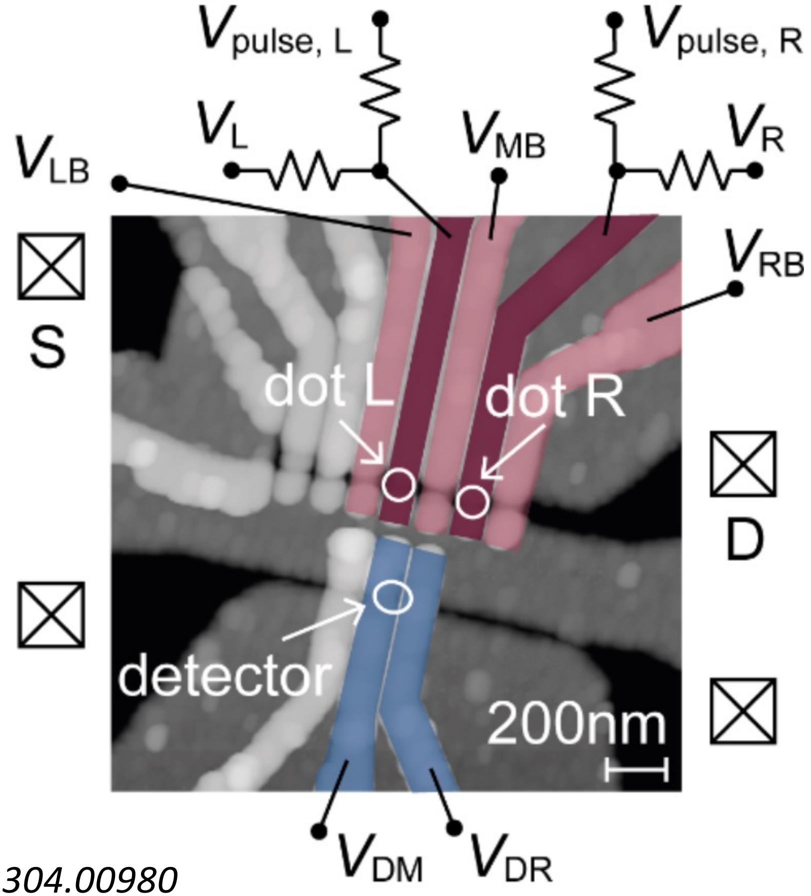

Garreis, R. and Tong C. *et al, arXiv:2304.00980*

Pulsing scheme for T_1-time measurement

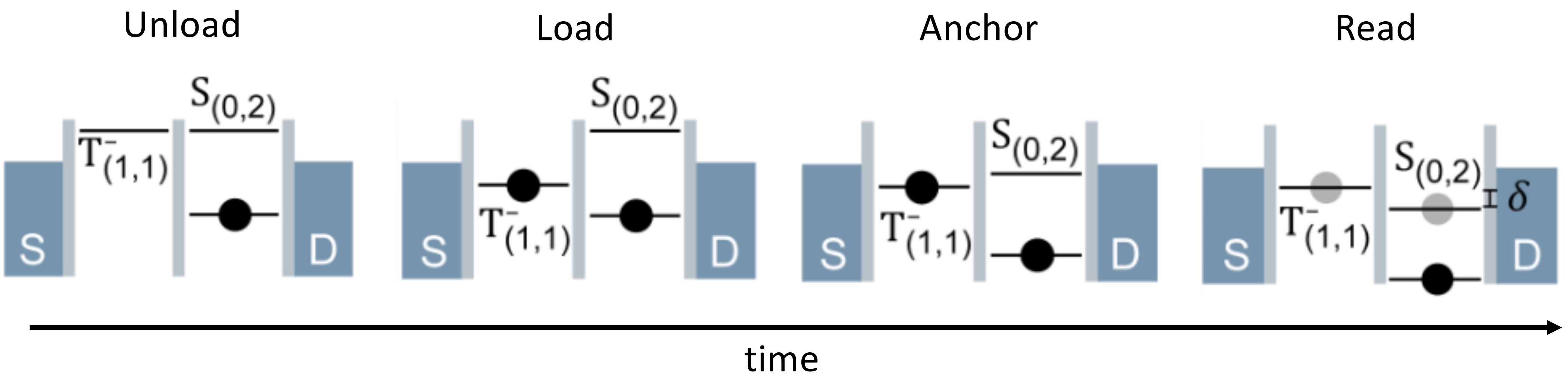

use charge sensor
to detect
(1,1) ↔ (0,2) transition
times

Garreis, R. and Tong C. *et al, arXiv:2304.00980*

Measured relaxation times

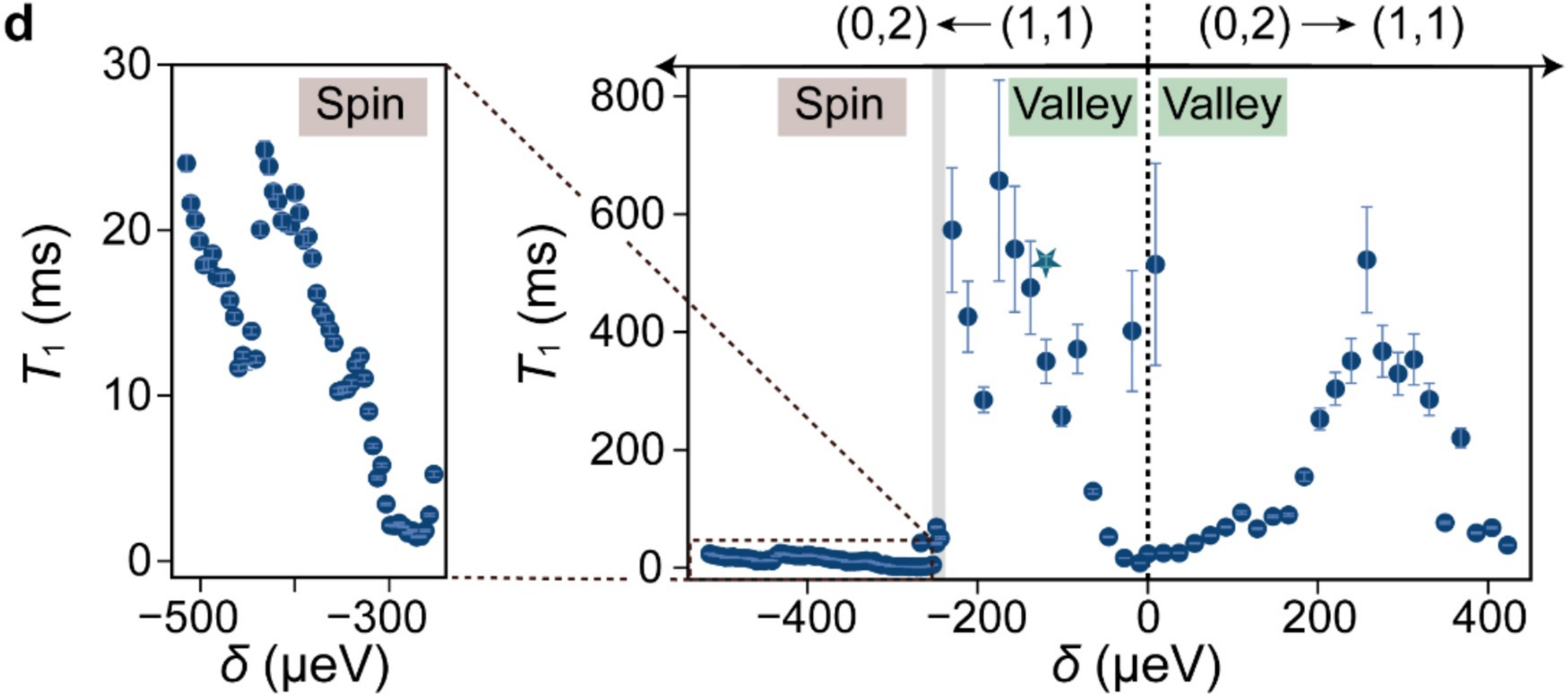

Garreis, R. and Tong C. *et al, arXiv:2304.00980*

Largest valley relaxation time: $\boxed{T_1 = 680\,\mathrm{ms}\ \text{ at }\ B = 250\,\mathrm{mT}}$

Dependence of relaxation times on tunnel coupling

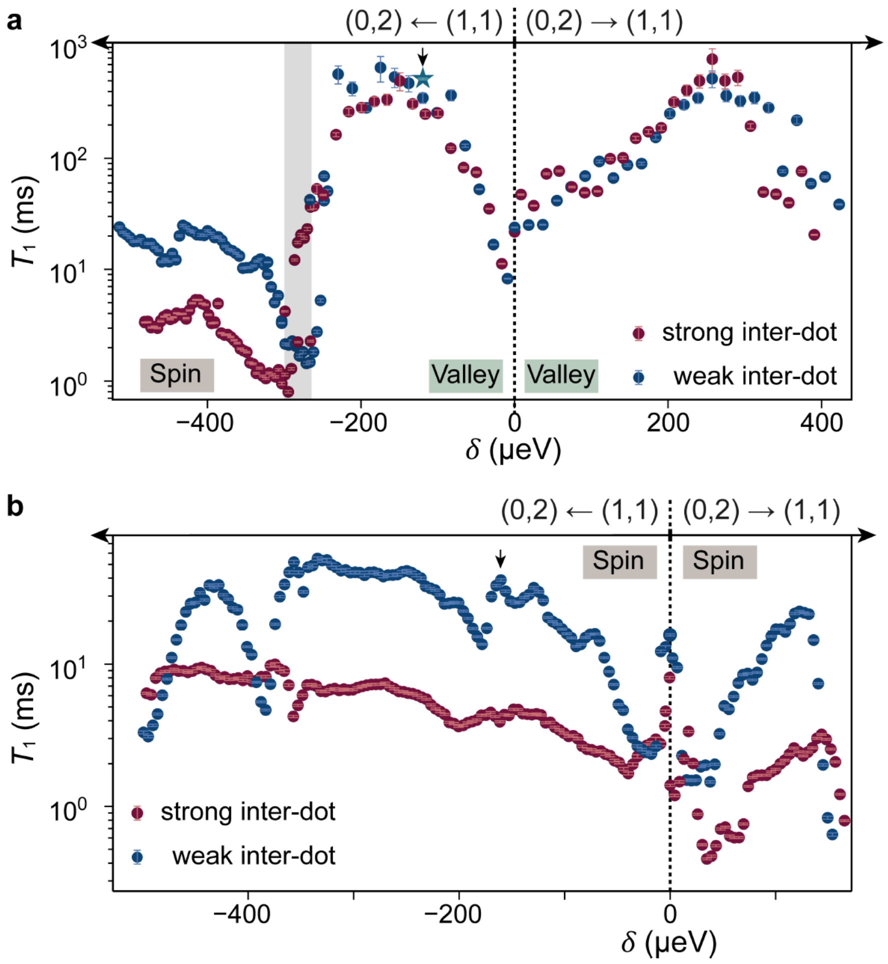

$$B = 250\,\mathrm{mT}$$

$$B = 700\,\mathrm{mT}$$

Garreis, R. and Tong C. *et al, arXiv:2304.00980*

What next?

- Measurement of T_2 times
- Hybrid devices coupling DQD to superconducting CPW-resonator
- Proximity induced spin-orbit interaction using TMDCs

Summary

- Gate-defined bilayer graphene quantum dots and their states

Tunable valley g-factor 20-80, Spin orbit coupling 73 μeV
Two-electron ground state is spin triplet
Magnetic field dials between Pauli valley- and spin-blockade

- Spin relaxation times in single quantum dots

Spin relaxation times up to 50 ms

- Valley relaxation times in double quantum dots

Valley relaxation times up to 650 ms at 1.7 T